AD-A172 488 STRESS STATE AND HYDROGEN-RELATED FRACTURE(U) 1/1
PENNSYLVANIA STATE UNIV UNIVERSITY PARK DEPT OF
MATERIALS SCIENCE AND ENGINEERING D A KOSS ET AL.
UNCLASSIFIED SEP 86 TR-2 N00014-86-K-0381 F/G 11/6 NL

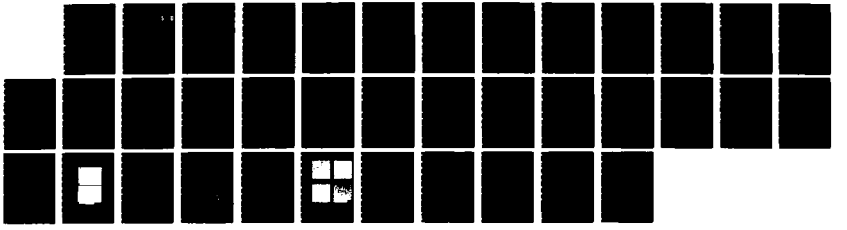

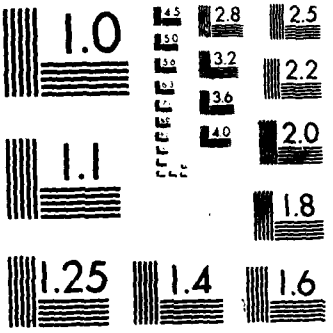

TECHNICAL REPORT NO. 2

TO

THE OFFICE OF NAVAL RESEARCH
CONTRACT NO. N00014-86-K-0381

STRESS STATE AND HYDROGEN-RELATED FRACTURE

D. A. KOSS AND FAN YUNCHANG

DEPARTMENT OF MATERIALS SCIENCE AND ENGINEERING
THE PENNSYLVANIA STATE UNIVERSITY
UNIVERSITY PARK, PA 16802

SECURITY CLASSIFICATION OF THIS PAGE *(When Data Entered)*

REPORT DOCUMENTATION PAGE	READ INSTRUCTIONS BEFORE COMPLETING FORM
1. REPORT NUMBER: Report No. 2 — 2. GOVT ACCESSION NO.: AD-A172488	3. RECIPIENT'S CATALOG NUMBER
4. TITLE *(and Subtitle)*: Stress State and Hydrogen-Related Fracture	5. TYPE OF REPORT & PERIOD COVERED
	6. PERFORMING ORG. REPORT NUMBER
7. AUTHOR(s): D. A. Koss and Fan Yunchang	8. CONTRACT OR GRANT NUMBER(s): N00014-86-K-0381
9. PERFORMING ORGANIZATION NAME AND ADDRESS: Dept. Materials Science and Eng. The Pennsylvania State University University Park, PA 16802	10. PROGRAM ELEMENT, PROJECT, TASK AREA & WORK UNIT NUMBERS
11. CONTROLLING OFFICE NAME AND ADDRESS: Office of Naval Research 800 N. Quincy Street Arlington, VA 22217	12. REPORT DATE: September, 1986 13. NUMBER OF PAGES: 33
14. MONITORING AGENCY NAME & ADDRESS*(if different from Controlling Office)*	15. SECURITY CLASS. *(of this report)*: Unclassified 15a. DECLASSIFICATION/DOWNGRADING SCHEDULE

16. DISTRIBUTION STATEMENT *(of this Report)*

Distribution of this document is unlimited.

17. DISTRIBUTION STATEMENT *(of the abstract entered in Block 20, if different from Report)*

18. SUPPLEMENTARY NOTES

19. KEY WORDS *(Continue on reverse side if necessary and identify by block number)*

Stress state, hydrogen embrittlement, fracture, Ti, Zircaloy-Z, Steels, Nickel

20. ABSTRACT *(Continue on reverse side if necessary and identify by block number)*

The influence of externally imposed stress state on the hydrogen-assisted fracture of metals is reviewed. Independent of any transport process which may result in hydrogen accumulation, the effects of stress state are to accelerate the hydrogen-related fracture processes with increasing triaxiality of stress state. The magnitude of the intrinsic sensitivity of hydrogen embrittlement to stress state effect depends on the mechanism of embrittlement. The behavior of selected hydride as well as non-hydride forming alloy systems is reviewed.

DD FORM 1 JAN 73 1473 EDITION OF 1 NOV 65 IS OBSOLETE

SECURITY CLASSIFICATION OF THIS PAGE *(When Data Entered)*

STRESS STATE AND HYDROGEN-RELATED FRACTURE

D. A. Koss[+] and Fan Yunchang[o]

[+]Dept. Materials Science and Eng.
The Pennsylvania State University
University Park, PA 16802

[o]Shiziazhuang Coal Mining Machinery Factory
11 Yuezin Road
Shiziazhuang City, Hebei, PRC

ABSTRACT

The influence of externally imposed stress state on the hydrogen-assisted fracture of metals is reviewed. Independent of any transport process which may result in hydrogen accumulation, the effects of stress state are to accelerate the hydrogen-related fracture processes with increasing triaxiality of stress state. The magnitude of the intrinsic sensitivity of hydrogen embrittlement to stress state effect depends on the mechanism of embrittlement. The behavior of selected hydride as well as non-hydride forming alloy systems is reviewed.

INTRODUCTION

The adverse effects of hydrogen on the mechanical behavior is well known and has been reviewed extensively; for example, see refs. 1-3. It is also generally accepted that the extent of the embrittlement becomes more severe in the presence of a notch or crack. This effect is usually associated with the gradient in mean or hydrostatic stress, which results in the transport of the hydrogen in solution such that it concentrates in regions of high hydrostatic stress. In addition, in hydride-forming systems the inhomogeneous stress field near a crack-tip usually decreases the free energy of the hydride relative to the solid solution, and hydride formation is possible near cracks, especially

when subjected to mode I loading.

Both of the above factors are well established causes of the increased susceptibility to hydrogen embrittlement of notched or cracked structural components. However, studies based on sheet metals subjected to uniform externally imposed stress states ranging from uniaxial to equibiaxial tension indicate that the fracture mechanisms for several different forms of hydrogen-assisted fracture are intrinsically sensitive to stress state. Early hints of such behavior came from disc pressure tests which showed that the burst pressure of clamped discs of certain materials was quite senitive to whether the pressurizing medium was gaseous helium of hydrogen[4]. Subsequently, a comparison of the behavior of steel specimens subjected to a range of test conditions indicated that the maximum principal stress required for failure was less for biaxially stressed discs than for uniaxially stressed bars[5,6]. Detailed studies applying test techniques common to sheet metal formability to hydrogen-charged sheet specimen have been recently conducted on several materials exhibiting a range of the forms of hydrogen embrittlement[7-11]. In these tests, the macrosiopic stress states can be systematically varied over nearly the complete range characterized by sheet thinning[12]. In all of the embrittlement forms examined, the sensitivity is such that, at a given hydrogen concentration, the fracture process is accelerated with an increase in the degree of biaxiality of the stress state. Thus, independent of stess- or strain-assisted hydrogen accumulation, hydrogen embrittlement should be most severe under strongly triaxial states of stress. The purpose of this review is to describe the existing evidence for such behavior and to examine the stress state effects in terms of the mechanisms of embrittlement.

DISCUSSION

The underlying causes for the intrinsic sensitivity of hydrogen embrittlement to externally imposed stress state depends on the embrittling mechanism and thus differs among materials. In order to analyze these effects, it is convenient to separate the fracture mechanisms on the basis of whether or not (a) hydrides are present and (b) there is a hydrogen-induced change in fracture mechanism.

(a) Hydride-forming Metals

If hydrides are present, due to either thermal or stress-assisted nucleation, hydrogen embrittlement usually involves a ductile fracture process based on accelerated void nucleation due to strain-induced hydride cracking. This is especially true in hydride forming metals such as Ti-, Nb-, Ta-, or Zr-based alloys; these normally contain few, if any, inclusions which otherwise would readily form voids. An intrinsic effect of stress state on embrittlement of a hydride forming system is expected to the extent that any or all of the stages of ductile fracture [void nucleation, void growth, and void linking] are affected by stress state. As will be shown below, the combination of hydrides and multiaxial tensile stress states facilitates both void nucleation and linking, thus enhancing embrittlement.

Evidence for the influence of stress state on the hydrogen embrittlement of Zircaloy-2 sheet is shown in Fig. 1 in the form of a fracture limit diagram[8]. Figure 1 indicates the major and minor principal (true) strains, ε_1 and ε_2, in the plane of the sheet at fracture. The value of ε_1 is determined by measurements of the width strain ε_2 and thickness strain ε_3 at the fracture surface and by calculating the magnitude of ε_1 assuming conservation of volume: $\varepsilon_1 = -(\varepsilon_2 + \varepsilon_3)$. As shown in Fig. 3, the ductility of the Zircaloy-2 sheet decreases at all levels of hydrogen as the degree of biaxiality of stress state increases.

However, the most significant feature is that the decrease of ductility with increasing hydrogen content is most severe as equibiaxial tension is approached. This trend is confirmed if the equivalent strains at fracture $\bar{\varepsilon}_f$ are determined at the various stress states and hydrogen levels[8]. Although these data also show a decrease in ductility with increasing hydrogen content for all stress states, the decrease is greatest in equibiaxial tension. Thus, as observed in Ti,[7,12] the hydrogen embrittlement of Zircaloy-2 sheet depends intrinsically on stress state, being the greatest under conditions of equibiaxial tension and high hydrogen contents. Furthermore, fractography indicates that a ductile, miciovoid fracture process occurs at over the range of hydrogen contents and stress states.

In order to understand the above results, it is very instructive to consider ductile fracture as a sequence consisting of void nucleation, void growth, and void linking. The influence of hydrogen and stress state on each of these stages is considered next.

Several studies have clearly established that fractures of hydride precipitates are the cause of hydrogen embrittlement in hydride-forming metals[1] and that fracture of hydrides is encouraged by an elevation of the triaxiality of the stress state[13]. As an example of these observations, Figure 2 shows that deformation causes hydride fracture and, in most instances, subsequent void nucleation along the fracture in the hydride platelet. Although voids usually form as a result of the fracture of hydrides normal to their length, failure of hydrides by a shear process also occurs, but this usually does not cause voids. An influence of stress state on the alignment of hydrides which fracture is also suggested in Fig. 2. In uniaxial tension, most of the fractures in those hydrides which are aligned parallel to the major principal strain axis. However, in the plane of the sheet, the major principal strain axes are

multidirectional in equibiaxial tension, and all orientations of hydride platelets in this plane appear equally susceptible to failure. Thus multiaxial tensile deformation should enhance void nucleation if for no other reason than a greater portion of hydride platelets are aligned parallel to an ε_1 axis and are in a favorable orientation for fracture when there are "multiple" tensile strain axes present.

A common notion is that hydrides cause embrittlment because they are brittle. Data in Figs. 3 and 4 show that considerable macroscopic plastic strain ($\bar{\varepsilon} > 0.2$) occurs in zirconium hydrides before an appreciable density of fractured hydrides ($10^2/mm^2$) is evident.* While bulk zirconium and titanium hydrides are usually brittle at room temperature (for a review, see ref. 14), it is highly unlikely that such large strains could be accomodated without plastic deformation of the hydride precipitate particles. For the plate-like hydride particles to remain elastic, very large incompability deformation which would have to occur within the matrix in order to accomodate strains in excess of 0.2 prior to hydride fracture. On the other hand, the hydride platlets are usually free of large angle grain boundaries, which would severely limit deformation, or surface flaws, which would readily initiate cracks, and appear to be subject to a stress state of nearly pure shear when embedded in a plastic matrix[7]. Thus it is very likely that hydride precipitates must be ductile, although their capacity to deform is sufficiently limited so as to be the primary cause for void formation[7,8].

Figures 3 and 4 show that the critical strain $\bar{\varepsilon}_N$ to nucleate the

*At a magnification of 1000 X, 10^2 voids/mm^2 correspond to 1 fractured hydride in an area 10 x 20 cm, or given typical void sizes, an area fraction of voids of about 3×10^{-4}.

detectable void density decreases with increasing hydrogen content as well as degree of biaxiality of stress state. This effect is most apparent at equibiaxial tension of the Ti at high hydrogen contents where $\bar{\varepsilon}_N \simeq 0.5$ at 60 ppm H but drops to $\bar{\varepsilon}_N \simeq 0.2$ at 960 H[7]. Thus, the combination of hydrides and multiaxial tensile stresses promotes void formation at increasingly small strains.

The role of stress state in fracturing the hydrides and nucleating voids may be understood by assuming that (a) hydride fracture obeys a maximum normal stress criterion and (b) the stresses σ_{ij}^{p} within the hydride may be estimated by utilizing the Beremin analysis[15]. In that analysis, the magnitude of σ_{ij}^{p} is a sum of a macroscopic stress component α_{ij}^{m} transferred to the particle and a "microscopic" component due to the inhomogeneity of strain between the matrix ε_{kl}^{m} and the particle ε_{kl}^{p}. According to the analyses, the stresses within the particle are given by the relationship:

$$\sigma_{ij}^{p} = \sigma_{ij}^{m} + \frac{2}{3}\frac{\bar{\sigma}^{m}}{\bar{\varepsilon}^{m}}(S_{ijkl}^{-1} - I_{ijkl})(\varepsilon_{lk}^{m} - \varepsilon_{kl}^{p}) \qquad (1)$$

where σ_{ij}^{m} and ε_{kl}^{m} are the stress and strain states respectively in the matrix, $\bar{\sigma}^{m}$ and $\bar{\varepsilon}^{m}$ are the equivalent stress and strains in the matrix, and S_{ijkl}^{-1} and I_{jkl} are respectively the Eshleby tensor and a unit tensor. Equation (1) may be evaluated assuming that the stresses and strains are homogeneous in the particle as well as in the matrix, that $d\bar{\sigma}^{m}/d\bar{\varepsilon}^{m}$ is a constant, and that the matrix-particle interaction is formulated from deformation theory of plasticity. It should be noted that hydride forming materials are often plastically anisotropic and an approrpriate yield criterion and the associated flow rule must be used. A limitation to the analysis is that strain gradients already exist near the hydride particles during their

nucleation and growth because of the size misfit of the hydrides; the strain gradients add internal stresses which are unknown in magnitude.

A complete evaluation of Eq. (1) requires knowledge of the relationship between deformation within the matrix and that within the particle [i.e. the $\varepsilon^{m}_{kl} - \varepsilon^{p}_{kl}$) tensor in Eq. (1)]. The maximum value of this tensor is when $\varepsilon^{m}_{kl} >> \varepsilon^{p}_{kl}$, in which case Beremin show that the equivalent strain to nucleate a void $\bar{\varepsilon}_N$ by particle fracture at a critical internal stress σ_c is

$$\bar{\varepsilon}_N = (\lambda E_p)^{-1}[\sigma_c - \sigma_1] \qquad (2)$$

where λ is a constant which depends on particle shape and strain path, $E_p = d\bar{\sigma}^{m}/d\bar{\varepsilon}^{m}$ of the matrix, and σ_1 is the maximum principal stress in the matrix. Assuming the hydride has a disc shape, given the imposed strain paths, and basing values of E_p on the multiaxial stress-strain behavior, the values of $(\lambda E_p)^{-1}$ may be estimated[7]. Of special note is that these calculations indicate that the magnitude of $(\lambda E_p)^{-1}$ is only weakly dependent on stress state for hydrides whose major axis is parallel to the major principal strain axis[7]. This suggests that, at a given strain, hydrides aligned with the ε_1 axis will experience similar maximum principal stresses roughly independent of loading path. It is possible to compare Eq. 2 with experimental data, and agreement between the observed strain for the nucleation of hydride fractures and Eq. 2 is quite good for Ti-H strained over a range of strain paths from uniaxial to equiliaxial tension[7]. That correlation indicates that larger hydrides tend to fail at a smaller critical normal stress and that some plastic strain in the hydrides occurs prior to their failure.

Equation 2 also indicates a dependence of $\bar{\varepsilon}_N$ on σ_1, the maximum principal stress in the matrix. In the case of materials such as Ti or Zr alloys, σ_1 may

be quite sensitive to deformation path due to the plastic anisotropy. At least in the case of Ti sheet, this appears to be the dominant factor in causing $\bar{\varepsilon}_N$ to decrease from uniaxial to plane-strain or equibiaxial tension of sheet material[7]. Attempts to test such a suggestion by testing "plastically isotropic" Ti sheet have been made but the resulting data were complicated by processing-induced changes of grain size and its effect on hydrogen embrittlement[16].

The influence of grain size on the hydrogen embrittlement of Ti has also been shown to depend on stress state[16]. The effect is such that the deleterious effect of large grain sizes on the susceptibility to hydrogen embrittlement is more severe in equibiaxial tension than in uniaxial tension. This apparently related to an increased ease of void nucleation as well as linking. Void nucleation should be enhanced as the large grains create conditions for large hydrides[17] which in turn fracture and form voids at smaller strains at the large normal stresses required to deform plastically anisotropic sheets in equibiaxial tension[7]. Void link-up should also be enhanced as the large, interconnected, and plate-like hydrides create paths for especially easy void link-up when subjected to the multidirectional major principal stresses in equibiaxial tension. These effects should be even more pronounced under triaxial states of stress, such as near notches or cracks, provided that the stress state is sufficiently long range to encompass several large grains/hydrides, thus permitting enhancement of both void nucleation and link-up.

The effects of externally imposed stress state on second stage of ductile fracture, void growth, is well known. Data[8] on hydrided Zircaloy-2 confirms the expected increase[18] in strain-induced void growth as the plastic contraint ratio $\sigma_H/\bar{\sigma}$ increases; note that $\sigma_H = 1/3(\sigma_1 + \sigma_2 + \sigma_3)$ is the hydrostatic or mean stress component. Given that comparatively little hydrogen is soluable at low

temperatures in the hydride-forming alloys and that multi-axial stress-strain behavior is largely unaffected by hydrogen in these alloys [at least in Ti-H alloys[19]], we expect void growth also to be unaffected by hydrogen content. Data for hydrogen charged Zircaloy-2 indicate this to be the case[8]. Thus enhanced void growth at large triaxial stresses will result in a decrease in fracture strain which should be independent of hydrogen contents in hydride forming alloys.

The third stage of ductile fracture, void linking, appears to be sensitive to hydrogen content and especially to stress state in hydride-forming metals. In Ti and Zr alloy sheet, increasing the biaxiality of stress state has a large effect in decreasing the fractured hydride/void density necessary to trigger void linking[7,8]. This appears to be a consequence of two factors: (a) given the multidirectional nature the two principal stresses in an equibiaxial stress field, large fraction of previously unfractured hydrides can directly participate in providing a fracture path which links the existing voids; the enhancement of void linking by hydride failure is especially effective when failure occurs at or near the "flat" faces of the hydride platlets and (b) the plastic instability process which triggers massive void linking appears to be initiated at smaller void densities in biaxial or triaxial tension[20,21]. Thus, the critical void density at the onset of void linking should decrease with increasing biaxiality/triaxiality of stress states.

In summary, the discussion above clearly indicates that hydrogen embrittlement in hydride-forming metals should be intrinsically senitive to stress state. Assuming a ductile fracture process, this effect is a consequence of both hydride fracture/void nucleation and void linking being accelerated by increasing biaxiality (or triaxiality) of stress state and increasing hydrogen content. It may be noted that these effects are related to the "damage" aspects

of ductile fracture as opposed to any aspects related to hydrogen-induced changes in flow behavior, which appear to be insignificant in hydride-forming alloys.

(b) Non-hydride Forming Metals

In alloys which do not readily form hydrides, hydrogen embrittlement is manifested by either an acceleration of the existing fracture process or a transition to a different mode of fracture. An example of the former is spheroidized plain carbon steels while among the latter are nickel, which can fail by an intergranular mode in the presence of hydrogen, and high strength steels, which may exhibit cleavage fracture induced by hydrogen. These cases will be discussed in the subsequent section.

i) No transition in fracture mode: Spheroidized plain carbon steels

The effects of hydrogen on the microstructural events involved in the ductile fracture of low to medium strength steels have received considerable attention. Extensive studies have been performed on the hydrogen embrittlement of spheroidized low to high carbon steels in tension and bend tests[for example, see refs. 22-25]. Although there is still some lack of agreement as to the precise influence of hydrogen on the specific stages of the fracture pocess, the data indicate that hydrogen enhances void nucleation at least at large strains. Some of the data also suggest hydrogen accelerates void growth, but the likelihood of internal pressurization causing enhanced growth is discounted due to the limited amount of hydrogen present[23,26]. Existing results for the influence of hydrogen on void linking remain inconclusive, although inferences have been made that void linkage is also enhanced by hydrogen[24]. Finally, there are well established instances of hydrogen-induced softening of iron[27] and of plastic instabilities which develope near the root of notches during straining when hydrogen is present.[25,28,29] Thus there are several "opportunities" by

which stress state may affect hydrogen embrittlement for the case where ductile, microvoid fracture is accelerated by hydrogen with no change in fracture mode.

Using the hydrogen embrittlement of spheroidized plain carbon steel sheets [AISI 1020, 1050, and 1070] as a model system for the acceleration of a ductile fracture process by hydrogen, Fan has investigated the influence of stress state over a range from uniaxial to equibiaxial tension[11]. Fig. 5 shows that, for a given stress state, data based on locally determined fracture strains show a decrease in ductility for the cathodically charged specimens when compared with those from the corresponding uncharged condition. The loss of ductility caused by hydrogen increases with an increasing degree of biaxiality of the stress state and volume fraction of spheroidized carbon particles (or carbon content). Thus, hydrogen embrittlement of spheroidized steel sheets, while not severe, is most prominent at high carbon contents and under an equibiaxial state of stress.

Metallographic and fractographic examinations show that the fracture of both charged and uncharged materials is a consequence of strain-induced void nucleation (due to carbide particle-ferrite matrix decohesion as in Fig. 6), void growth, and void link-up. The quantitative determination of void density, void size, and void areal fraction as a function of the equivalent plastic strain indicates that both void nucleation and void growth are accelerated by hydrogen, especially in equibiaxial tension[11]. Fig. 7 shows an example of the void density data as a function of equivalent strain for 1020 steel. The data are corrected for void growth using a technique described elsewhere.[30] Both the raw data and the corrected void nucleation data show that hydrogen facilitates void nucleation especially at large strains and under equibiaxial tension. Similar behavior is observed in the 1070 steel.

The comparative ease of void formation may be examined in terms of the critical strain for void nucleation, ε_N. Defining ε_N as the equivalent strain

at which a void density of 0.8×10^4 voids per mm^2 is present, the data show ε_N to be decreased by cathodically charged hydrogen at least in equibiaxial tension (see Fig. 7)[11]. The effect of hydrogen on void formation is more severe in equibiaxial tension than in uniaxial tension, and more pronounced in the high carbon steel than in the low carbon steel[11]. For example, the critical strain, $\varepsilon_N = 0.2$ is observed for the hydrogen-charged specimen of the 1070 steel under equibiaxial tension while for the corresponding uncharged specimen the critical strain ε_N is about 0.4. In contrast, under uniaxial tension state, the critical strain ε_N for charged and uncharged specimens are very similar in magnitude although $(\varepsilon_N)_{w/H}$ is still smaller than $(\varepsilon_N)_{w/o}$. In the low carbon steel AISI 1020, increasing the biaxiality of the loading path also enhances the influence of hydrogen on the critical void nucleation strain but the effect is smaller than that in high carbon steel.

Another important parameter in ductile fracture process is the critical void density ρ_c at which massive void linking is triggered at a void profusion strain and final separation of the fracture surfaces occurs. This parameter provides a quantitative measurement of the fraction of particles involved in void nucleation, assuming that each void is associated with one carbide particle in spheroidized carbon steels. For the 1070 steel, the critical void density ρ_c is decreased by hydrogen for both uniaxial and equibiaxial tension[11]. In contrast, as may be seen in Fig. 7, in the low carbon 1020 steel the critical void density ρ_c for hydrogen-charged specimens is higher than that for the uncharged specimens. This behavior of the low carbon steel is similar to that observed by Cialone and Asaro in the 1020 and 1045 steels[26]. Although the inverse effect in low carbon steel is perplexing, some insight ay be obtained by examining the data in terms of the void nucleation model proposed elsewhere[29]. In Fig. 7, an apparent saturation of the <u>rate</u> of void density increase is

observed in the 1020 steel as the plastic strain approaches the fracture strain. This saturation can be explained in terms of an exhaustion of the available supply of void nucleation sites at strains near fracture[29]. The higher saturation plateau in the charged specimens of the 1020 steel is consistent with a reduced critical particle size for void formation in the presence of hydrogen. In contrast, fracture by void linking apparently occurs in the 1070 steel prior to an exhaustion of void nucleation sites. This may be due to the very high carbide density and small ferrite mean free path in steel 1070 causing voids to link at strains smaller than that for void density saturation. The large spatial separation of carbide particles in the 1020 steel allows voids to grow until void nucleation approaches saturation even in the presence of hydrogen and equibiaxial tension.

Void growth rates as a function of stress state have been determined both in terms of the ratio of void size d at a plastic strain ε to a chosen initial void size d_o (d_o = 0.50μ m in steel 1020 and d_o = 0.25μ m in steel 1070) at a corresponding plastic strain ε_0[11]. The ratio , d/d_o, is shown as a function of the equivalent strain increment ($\varepsilon-\varepsilon_o$) in Fig. 8 for the 1020 steel. This figure, as well as similar data for the 1070 steel, shows an enhancement of void growth rate caused by cathodically charged hydrogen for specimens strained in equibiaxial tension. The effect of hydrogen on void growth is smaller in uniaxial tension for both the low and the high carbon steels. These data are very consistent with similar measurements of the average void area as a function of equivalent strain[11].

Void growth data also show that, except in the case of uniaxial tension of the 1020 steel, the void size at the fracture d_f appears to be reduced by hydrogen charging. As seen in Fig. 8, the extrapolated critical void size d_f for the charged specimens is about 20% smaller than that for the corresponding

uncharged specimens in both uniaxial and equibiaxial tension test of the 1020 steel. Similar data for the 1070 steel show that the critical void size is about 30% smaller in the charged punch specimen than that in the corresponding uncharged specimen. These results are generally in accordance with the qualitative observations of voids adjacent to the fracture surface.

In summary, these data show that both void nucleation and void growth is enhanced by hydrogen and increasing the biaxiality of stress state, especially at large strains. The effects of hydrogen on void linking is less obvious. The present evidence suggests that void size is decreased by hydrogen at the onset of final failure, but that void density is decreased only at high carbide densities. This suggests that void linking may be accelerated by hydrogen if the carbon content is sufficiently large to reduce intercarbide spacings to a level where the flow behavior in the ligaments between voids is significantly affected by hydrogen.

The mechanisms by which hydrogen exerts a stress-state sensitive influence on void nucleation and growth and possibly linking are not well established. In a steel which is nearly plastically isotropic, equibiaxial tension does not significantly increase the maximum principal stress σ_1 in Eq. 1, although a greater fraction of the carbide-matrix interface is subject to σ_1 in equibiaxial tension. This should result in a modest increase in void nucleation with increasing biaxiality of stress state, but probably not of the scale evidenced in Fig. 7. It may also be possible that the hydrostatic stress component σ_H enters directly into the criterion for void nucleation, as it does in some theories,[31] in which case void nucleation would be enhanced with increasing σ_H-values. A strain-path sensitivity of hydrogen sweep-in by dislocations also cannot be ruled out.

While hydrogen-accelerated void growth has been previously observed[23,28],

the internal pressure mechanism is generally discounted[23,26]. In the spheriodized steels, a possible cause of enhanced void growth is a local hydrogen-softening effect which may occur near the voiding carbide-matrix interfaces. Such an effect would be sensitive to the expected depletion of substitutional solute atoms near the carbides and would require an enhancement of hydrogen in solution near a growing void. The latter effect depends on at least some degree of reversibility of the trapping of hydrogen at carbide-matrix interfaces and the subsequent growing voids. A local dynamic enhancement of hydrogen in solution near a growing void, coupled with hydrogen-induced softening, could account for the observed hydrogen-enhanced void growth. If hydrogen-induced softening can occur on a local scale, then the plastic instability process which triggers void linking would certainly be enhanced. This may have some relationship to the shear instabilities observed in hydrogen-charged 1090 steel[25,28,29]. Thus, hydrogen embrittlement in these steels must be viewed from both damage and flow standpoints.

ii) Transition in Fracture Mode: Nickel

In certain nonhydride forming metals, hydrogen embrittlement is accompanied by a change in fracture mode. In the case of nickel, hydrogen induces (or aids in inducing) intergranular fracture. The hydrogen embrittlment of polycrystalline nickel, usually in the form of smooth uniaxial test bars, has been well characterized (see, for example, refs. 1, 31-36). It is clear from these studies that segregation of hydrogen to grain boundaries occurs, but the precise mechanism of resulting embrittlement is not established. Results of single crystal studies have also shown that in the presence of hydrogen, crack-tip plasticity is affected such that a high degree of slip localization occurs ahead of the crack-tip[1,35].

The influence of stress state on the intergranular hydrogen embrittlement of Ni sheet has been examined over a range of stress states which include (a) uniaxial tension, (b) plane-strain tension and (c) equibiaxial tension[37]. Taken together, these represent nearly the complete range of strain paths which result in sheet thinning.

The influence of the stress state on the hydrogen embrittlement of nickel sheet at an equivalent strain rate of 1.0×10^{-5} s^{-1} is shown in Fig. 9[37]. The loss of ductility data is presented in two forms of effective fracture strains in the H_2SO_4 environment normalized with respect to the uncharged (air) values. Figure 9a presents the normalized effective limit strain $\bar{\varepsilon}_H / \bar{\varepsilon}_{w/o\ H}$ which is based on the strains adjacent to the localized deformation or neck near the fracture surface. These limit strains indicate the magnitude of the strain at the onset of the localized flow instability which results in failure. Alternatively, Fig. 9b shows the ductility loss based on the principal strains of fracture measured directly from the 1 mm grids <u>at</u> the fracture surface. Thus, the $\bar{\varepsilon}^f$ data in Fig. 9b are related to reduction of area measurements in a tensile test while the ε^l data in Fig. 4a are akin to tensile elongation at failure. Figure 9 shows that both on the basis of $\bar{\varepsilon}^f$ and $\bar{\varepsilon}^\ell$ behavior, the degree of hydrogen embrittlement increases as the stress state tends from uniaxial to equibiaxial tension.

Several investigations have shown that HE of Ni is characterized by intergranular (I/G) fracture often mixed with transgranular, ductile fracture.[32,34,35] When viewed on the surface of sheet specimens undergoing deformation during charging, the I/G fracture is seen to be a consequence of profuse microcracking which occurs on the specimen surface exposed to hydrogen. Figure 10 shows that these microcracks, which tend to occur along grain boundaries oriented normal to the maximum principal stress, increase in density

with strain. As seen in Figure 10, while the total number of microcracks per unit area is always significantly greater in uniaxial tension than in equibiaxial tension, quantitative metallography indicates that the total crack length/area is roughly independent of stress state at a given equivalent shear strain. Consequently, the average crack length is greater in equibiaxial tension than in uniaxial tension at a given strain. Furthermore, examination of Fig. 10 shows that the presence of longer cracks in equibiaxial tension is a result of the link-up of microcracks into a "macrocrack". These data plus quantitative crack density and length data show that, while strain-induced microcrack link-up occurs in both uniaxial an equibiaxial tension, the rate of link-up is greater in equibiaxial tension[37].

The above behavior can be readily understood on the basis of a critical normal stress criterion $(\sigma_1)_c$ for intergranular (I/G) fracture. As implied by the previously discussed analysis[7,15], the critical stress normal to a grain boundary at its failure is primarily the sum of two components:

$$(\sigma_1)_c = (\sigma_1)_{micro} + (\sigma_1)_{macro} \qquad (3)$$

where $(\sigma_1)_{micro}$ is a normal stress component which develops on a microscopic scale and is a consequence of plastic incompatibilty between grains, and $(\sigma_1)_{macro}$ is the normal stress component transferred to the boundary from the macroscopic plasticity of the matrix.

One approach in evaluating Eq. 3 for a I/G hydrogen embrittlement process is to estimate $(\sigma_1)_{micro}$ on the basis of the simplification of Beremin.[14] This indicates that $(\sigma_1)_{micro} \alpha (\varepsilon^m_{ij} - \varepsilon^g_{ij})$ for an isolated grain,* independent of stress state for spherical grains in a plastically isotropic matrix. Thus,

*ε^m_{ij} and ε^g_{ij} are the strain components in the matrix and grain, respectively.

for example, the role of hydrogen in intergranular HE may be (a) to increase $(\sigma_1)_{micro}$ due to enhanced plastic incompatibility if dislocation sweeping[2,38] hydrogen and flow softening adjacent to the boundaries occur,[1] and/or (b) to decrease the critical normal stress at grain boundary failure $(\sigma_1)_c$ hydrogen sweeping causes a decrease in fracture strength of the boundary itself. In either event, strain-induced I/G fracture of isolated grain boundaries due to hydrogen embrittlemnt is a consequence.

The alignment of the microcracks normal to the major principal strain axis may also be interpreted in terms of a critical normal stress criterion. In the present case both $(\sigma_1)_{micro}$ and $(\sigma_1)_{macro}$ in Eq. 3 should be aligned nearly parallel with the axis of the major principal strain ε_1 imposed by the test. Thus, while the microcracks tend to be parallel to each other and normal to ε_1 in uniaxial and plane-strain tension, their orientation is random in the plane of the sheet in equibiaxial tension; see Fig. 10. In the latter case, this reflects the $\varepsilon_1 = \varepsilon_2$ strain path which is directed radially from the top of the dome in the equibiaxial punch-stretch deformation mode. The profile of the final fracture surfaces are also consistent with the above in that the fracture path (as projected onto the plane of the sheet) is much more tortuous in equibiaxial tension than in uniaxial or plane-strain tension.

Given the condition of normality between microcracks and the maximum principal strain direction, the ease with which microcracks link-up in equibiaxial tension is thus seen as simply a consequence of the "random" alignment of the $\varepsilon_1 = \varepsilon_2$ axes within the plane of the sheet during equibiaxial deformation[37]. The same effect causes the surface of sheet undergoing stress corrosion cracking to appear as "dried and cracked mud" when tested in equibaxial tension.[39] Because of the relative ease of microcrack link-up, the formation of long macrocracks occurs at increasingly smaller effective strains

as the biaxiality of the stress state increases. The subsequent growth of macrocracks results in failure.

In view of the above, it is concluded that the HE of nickel sheet is intrinsically sensitive to stress state[37]. The effect can be interpreted by using a critical normal stress criterion for I/G fracture and recognizing that grain boundaries may be randomly oriented in the plane of the sheet and still be subjected to large normal stresses in equibiaxial tension. The major consequence of this "randomness" of σ_1 effect is to accelerate the link-up of isolated grain-boundary microcracks into a macrocrack which then propagates, causing failure at smaller strains. Thus the HE of Ni sheet should be most severe in equibiaxial or triaxial tension.

iii) Transition in Fracture Mode: High Strength Steels

High steels exhibit a range of fracture modes in the presence of hydrogen. Frequently, cleavage or quasi-cleavage occurs although intergranular fracture is also common (for example, see ref. 40 and 41). The effect of stress state on the intrinsic sensitivity of hydrogen embrittlement in these such steels has not been studied. Recent data for hydrogen-induced crack growth in modes II and III indicates that hydrogen accumulation should occur, even under mode III loading if the strain field of the hydrogen atom in α-Fe exhibits non-spherical symmetry[42].

In view of the behavior of the other systems previously discussed, we may speculate as to the possiblity of hydrogen embrittlement in high strength steels being intrinsically sensitive to stress state steels. Firstly, both intergranular and cleavage fracture are sensitive to the maximum principal stress and thus any stress state which increases $\sigma_1/\bar{\sigma}$ is likely to enhance embrittlement. Furthermore, previous research indicates that crack nucleation

is a subsurface event which in all likelihood involves multiple microcrack sites (carbides, for example) which must link for fracture to occur[41]. Thus, as in the case of nickel, any multidirectional tensile stress state should enhance the microcrack linking process, given the increased density of potential fracture planes normal to σ_1. Both of these factors should increase the susceptibility of high strength steels to hydrogen embrittlement under conditions of triaxiality of the stress state, regardless of any hydrogen accumulation which may occur.

SUMMARY

The hydrogen embrittlement of a range of alloy systems is intrinsically sensitive to an externally imposed stress state. Independent of hydrogen accumulation, the effect of stress state is to accelerate the hydrogen-related fracture processes with increasing triaxiality of stress state. The causes for this effect depend on the mechanisms of embrittlement specific to each material and thus differ among the classes of materials. In view of the above and the well-known tendancy for hydrogen to accumulate in regions of high hydrostatic stress near notches or mode I cracks, the well-known severity of hydrogen embrittlement in stressed components which are notched or cracked may be understood.

ACKNOWLEDGEMENTS

The authors wish to express their appreciation to Drs. Heldt and R. Bourcier, Messrs. S. Kampe and D. Gerard, and Ms. B. Lograsso for many

stimulating discussions. This research was by the Office of Naval Research through Contract No. N00014-86-K-0381 and by the Department of Energy through Contract No. DE-AC0Z-81ER10941.

References

1. Birnbaum, H. K., Hydrogen Related Fracture of Metals in Atomistics of Fracture, Latanision, R. M. and Pickens, J. R. (ed.), New York, Plenum Press, 1983, p. 733-770.

2. Hirth, J. P. and Johnson, H. H., On the Transport of Hydrogen by Dislocations in Atomistics of Fracture, Latanision, R. M. and Pickens, J. R. (ed.), New York, Plenum Press, 1983, p. 771-788.

3. Thompson, A. W. and Bernstein, I. M., The Role of Metallurgical Variables in Hydrogen-Assisted Environmental Fracture in Advances in Corrosion Science and Technology, Fontara, M. G. and Staehle, R. (ed.), New York, Plenum Press, 1980, p. 53-175.

4. Fidelle, J. P., Bernardi, R., Broudeur, R., Roux, C. and Rapin, M., Disk Pressure Testing of Hydrogen Environmental Embrittlement in Hydrogen Embrittlement Testing, ASTM STP 543, Philadelphia, ASTM, 1974, p. 221-253.

5. Louthan, M. R., Sisson, R. D., and McNiff, R. P., Stress State and Thickness Effects on Delayed Failure in Hydrogen Effects in Metals, Thompson, A. W. and Bernstein, I. M. (ed., Warrendale, PA, AIME, 1980, p. 829-838.

6. Murali, J., Louthan, M. R., Sisson, R. D., and McNitt, R. P., Influence of Externally Imposed Constraint on the Hydrogen Embrittlement of Steels, in Current Solutions to Hydrogen Problems in Steels, Metals Park, OH, 1982, p. 394-403.

7. Boucier, R. J. and Koss, D. A., Hydrogen Embrittlement of Titanium Sheet Under Multiaxial States of Stress, Acta Met. 32, (1984) 2091-2099.

8. Fan Yunchang and Koss, D. A., The Influence of Multiaxial States of Stress on the Hydrogen Embrittlement of Zirconium Alloy Sheet, Metall. Trans. A, 16A, (1985) 675-681.

9. Lograsso, B. J., Boucier, R. J., and Koss, D. A., The Influence of Hydrogen on the Multiaxial Fracture Behavior of Titanium Alloy Sheets in Titanium Science and Technology, Germany, DGM, 1985, p. 2463-2469.

10. Kampe, S. L. and Koss, D. A., The Effect of Stress State on the Hydrogen Embrittlement of Nickel, Acta Met. 34, 1986 (55-61).

11. Fan Yunchang, The Hydrogen Embrittlement of Spheriodized Plain Carbon Steel Sheets Under Multiaxial States of Stress, PhD Thesis, Michigan Technological University, Houghton, MI, 1985.

12. Bourcier, R. J. and Koss, D. A., A Failure Limit Diagram for Determining Hydrogen Embirttlement of Sheet Under Multiaxial Loading Conditions, Scripta Met 16, (1982) 515-520.

13. Simpson, L. A., Criteria for Fracture Initiation at Hydrides in Zirconium -2.5% Noibium Alloy Metall. Trans. A, 12A, 1981 (2113-2124).

14. Birnbaum, H. K., Mechanical Properties of Metal Hydrides, Journal Less Common Metals 114, (31-41).

15. Beremin, F. M., Cavity Formation from Inclusions in Ductile Fracture of A508 Steel, Metall. Trans. 12A , 1981 (723-731).

16. Gerard, D. A. and Koss, D. A., The Combined Effect of Stress State and Grain Size on Hydrogen Embrittlement of Titanium, Scripta Met 19, 1985 (1521-1525).

17. Beevers, C. J., Warren, M. R. and Edmonds, D. B., Fracture of Titanium-Hydrogen Alloys J. Less Common Metals 14, 1968 (387-396).

18. Rice, J. R. and Tracey, D. M., On the Ductile Enlargement of Voids in Triaxial Stress Fields, J. Mech. Phys. Solids 17, 1969 (201-271).

19. Lentz, C. W., Stout, M. G., Hecker, S. S., and Koss, D. A., The Effect of Hydrogen on the Multiaxial Stress-Strain Behavior of Titanium Tubing", Metall. Trans. A., 14A, 1983 (2527-2533).

20. Marciniak, Z. and Kucznski, K., The Forming Limit Curve for Bending Processes, Int. J. Mech. Sci. 21, 1979 (609-621).

21. Saje, M., Pan, J., and Needleman, A. Void Nucleation Effects on Shear Localization in Porous Plastic Solids, Int. Journ. Fracture, 19, 1982 (163-182).

22. Oriani, R. and Josephic, P. H., Effects of Hydrogen on the Plastic Properties of Medium Carbon Steels, Metall. Trans A, 11A, 1980 (1809-1820).

23. Cialone, H. and Asaro, R. J., Hydrogen Assisted Fracture of Spheriodized Plain Carbon Steels, Metall. Trans A., 12A, 1981 (1373-1387).

24. Garber, R., Bernstein, I. M. and Thompson, A. W., Hydrogen Assisted Ductile Fracture of Spheroidized Carbon Steels, Metall. Trans. A. 12A , 225 (1981), 1981 (225-234).

25. Onyewuenyi, O. A. and Hirth, J. P., Effects of Hydrogen on Notch Ductility and Fracture of Spheroidized AISI 1090 Steels, Metall. Trans A, 14A, 1983 (259-269).

26. Cialone, H. and Asaro, R. J., The Role of Hydrogen in the Ductile Fracture of Plain Carbon Steels, Metall. Trans A, 10A, 1979 (367-375).

27. Kimura, H., Matsui, H., Kimura, A., Kimura, T., and Oguri K., Softening and Hardening in High Purity Iron and Its Alloys Charged with Hydrogen in Hydrogen Effects in Metals, Bernstein, I. M. and Thompson, A. W. (eds.), Warrendale, PA, TMS-AIME, 1981, p. 191-208.

28. Lee, T. D., Goldenberg, T., and Hirth, J. P., Effect of Hydrogen on Fracture of U-Notched Bend Specimens of Spheroidized AISI 1095 Steel, Metall. Trans. A, 10A, 1979 (199-208).

29. Oneyewuenyi, O. A. and Hirth, J. P., Plastic Instability in U-Notched Bend Specimens of Spheroidized 1090 Steel, Metall. Trans A, 15A, 1982 (2209-2218).

30. Fisher, J. R. and Garland, J., Void Nucleation in Spheroidized Carbon Steels, Metal Science, 15, 1981 (185-192).

31. Goods, S. H. and Brown, L. M., The Nucleation of Cavities by Plastic Deformation, Acta Met. 27 , 1979 (1-15).

32. Troiano, A. R., The Role of Hydrogen and Other Interstitials in the Mechanical Behavior of Metals, Trans. Am. Soc. Metals, 52, 1960 (54-80).

33. Latanision, R. M. and Opperhauser, H., The Intergranular Embrittlement of Nickel by Hydrogen: The Effect of Grain Boundary Segregation, Metall. Trans. 5, 1974 (483-492).

34. Smith, G. C., Effect of Hydrogen on Nickel and Nickel-Base Alloys, in Hydrogen in Metals, Bernstein, I. M. and Thompson, A. W. (eds.), Metals Park, OH, ASM, 1974, p. 485-511.

35. Eastman, J., Matsumoto, T., Narita, N., Heubaum, F., and Birnbaum, H., Hydrogen Effects in Nickel-Embrittlement or Enhanced Ductility in Hydrogen Effects in Metals, Bernstein, I. M. and Thompson, A. W. (eds.), Warrendale, PA, TMS-AIME, 1981, p. 397-410.

36. Bruemaner, S. M., Jones, R. H., Thomas, M. T., and Baer, D. R., Influence of Sulfur, Phosphorous, and Antimony Segregation on the Intergranular Hydrogen Embrittlement of Nickel, Metall. Trans. A, 14A, 1983, (223-232).

37. Kampe, S. L. and Koss, D. A., The Effect of Stress State on the Hydrogen Embrittlement of Nickel, Acta Met. 34, 1986 (55-61).

38. Tien, J. K., Nair, S. V. and Jensen, R. R., Dislocation Sweeping of Hydrogen and Hydrogen Embrittlement in Hydrogen Effects in Metals, Bernstein, I. M. and Thompson, A. W. (eds.) Warrendale, PA, TMS-AIME, 1981, p. 37-56.

39. Blanchard, W. K., Koss, D. A., Heldt, L. A., The Influence of Deformation Path on the Slow Strain Rate Stress Corrosion Cracking of Admiralty Brass Sheet, Metall. Trans. A, 15A, 1984, (1281-1286).

40. Bernstein, I. M. and Thompson, A. W., The Effect of Metallurgical Variables on Environmental Fracture of Steels, Int. Met. Rev. 21, 1976 (269-287).

41. Hirth, J. P., Effects of Hydrogen on the Properties of Iron and Steel, Metall. Trans. 11A, 1980 (861-890).

42. Chu, W. Y., Wang, Hi Li, and Hsiao, C. M., Corrosion 40, 1984 (487-92).

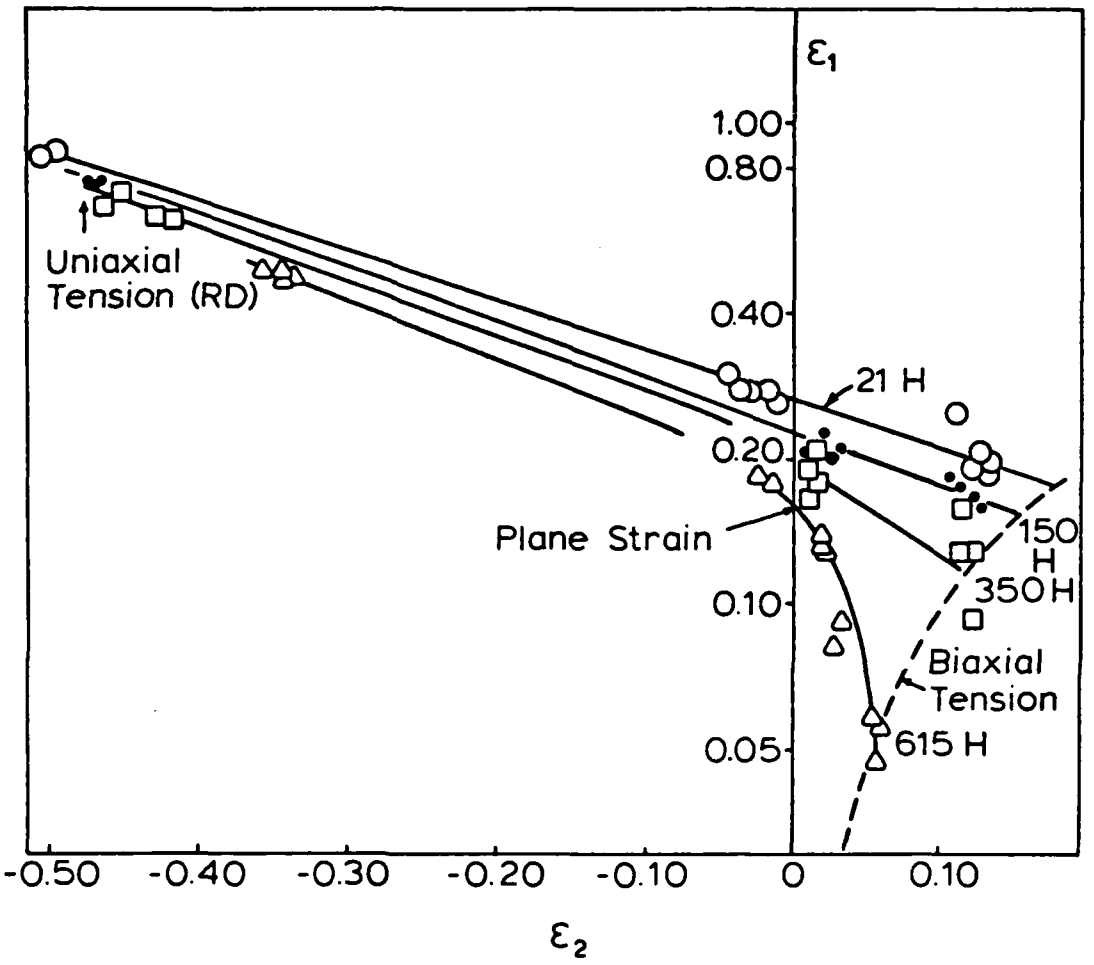

Figure 1: A fracture limit diagram for ZIRCALOY-2 sheet at four levels of hydrogen. The major ε_1 and minor ε_2 principal strains in the plane of the sheet at fracture are shown. After ref. 8.

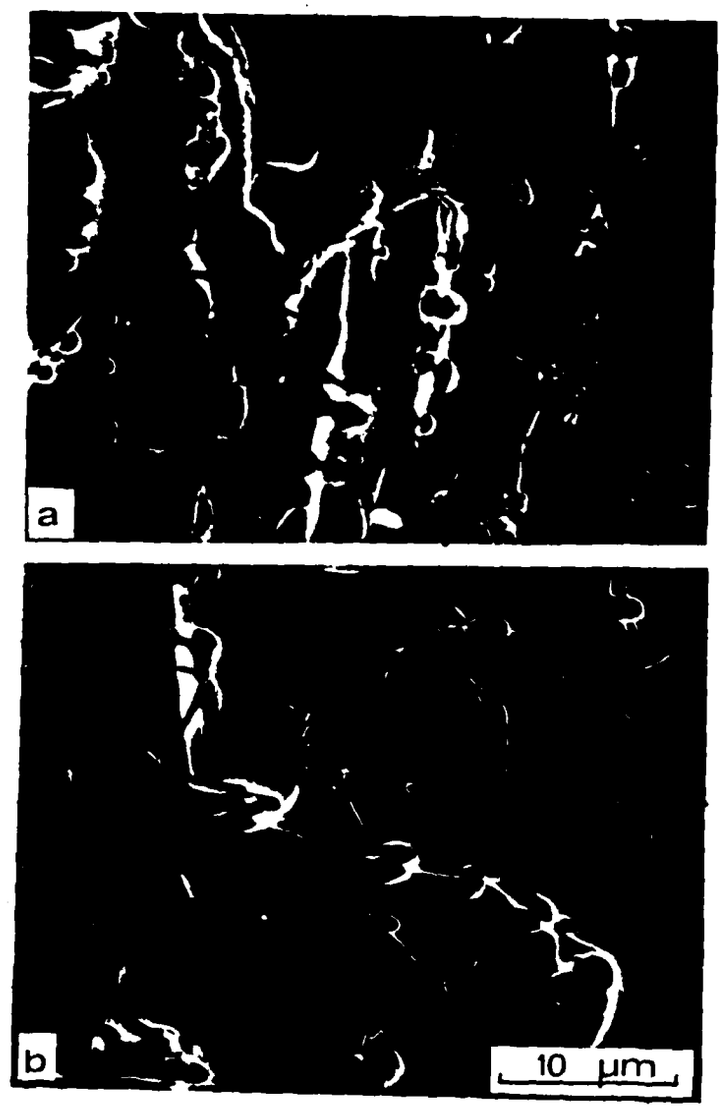

Figure 2: Electron micrographs showing strain-induced hydride fracture and void formation in titanium subjected to (a) uniaxial tension and (b) equibiaxial tension. After ref. 7.

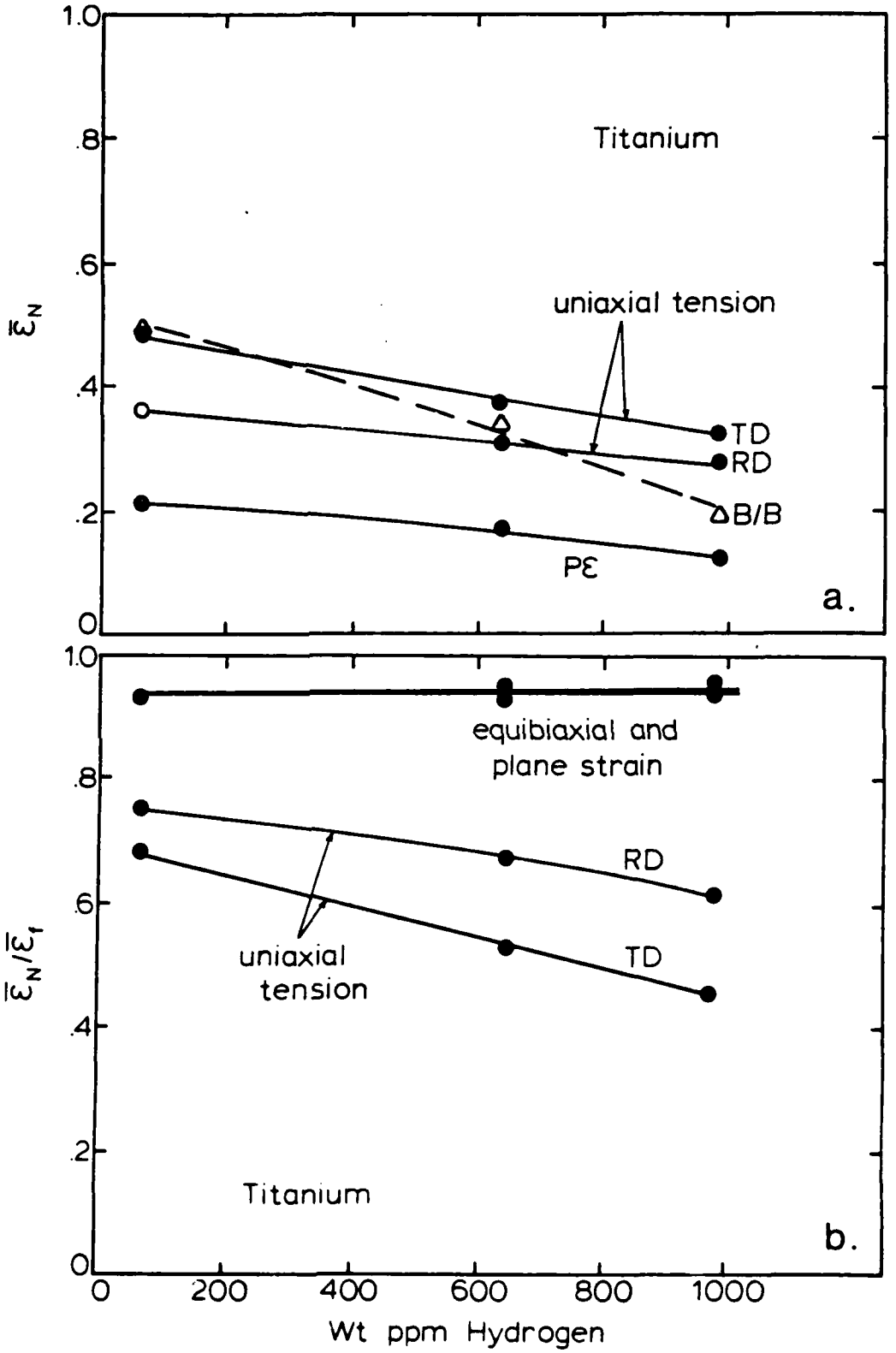

Fig. 3 - The influence of hydrogen on (a) the equivalent strain $\bar{\varepsilon}_N$ required to form 10^2 voids/mm^2 and (b) ratio of $\bar{\varepsilon}_N$ to the equivalent strain at fracture $\bar{\varepsilon}_f$. The terms TD and RD refer to uniaxial tensile deformation in the transverse and rolling directions, respectively while B/B and Pε denote balanced biaxial and plane strain tension, respectively. After ref. 7.

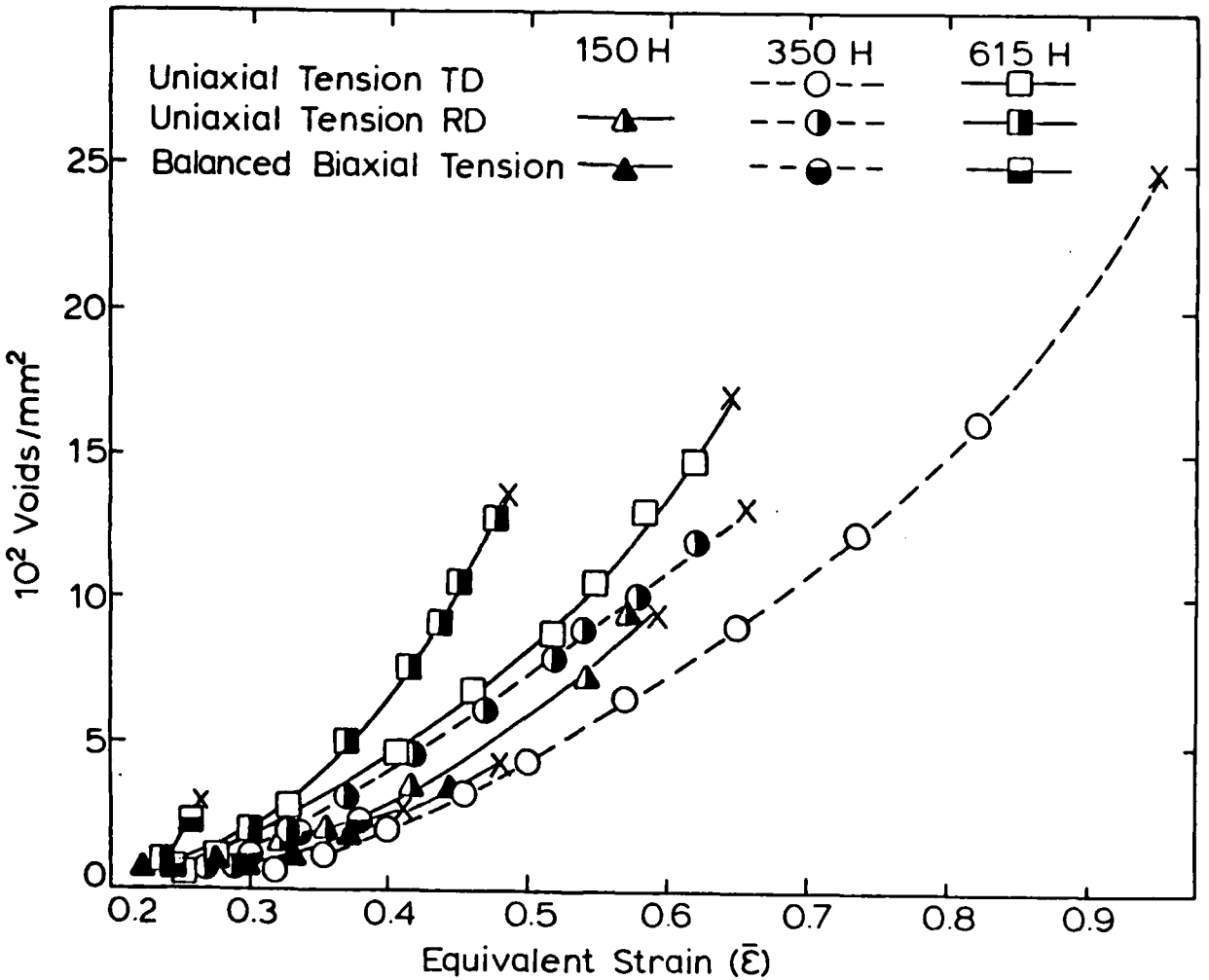

Figure 4: The dependence of void density on the Hill equivalent strain for Zircaloy-2 sheet deformed in either uniaxial or equibiaxial tension. Data are extrapolated to the fracture strain, marked x. All voids are associated with fractured hydrides. After ref. 8.

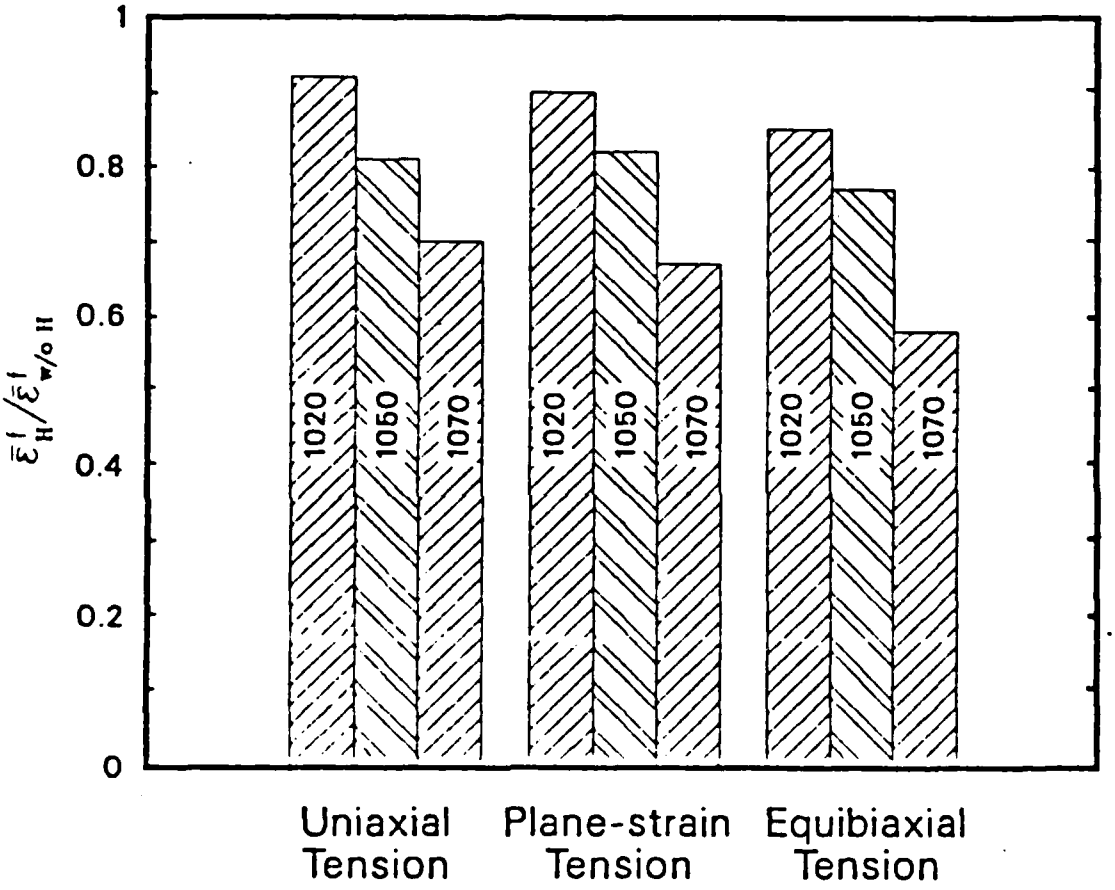

Figure 5: The dependence of hydrogen embrittlement of three spheroidized plain carbon steels as a function of stress state.

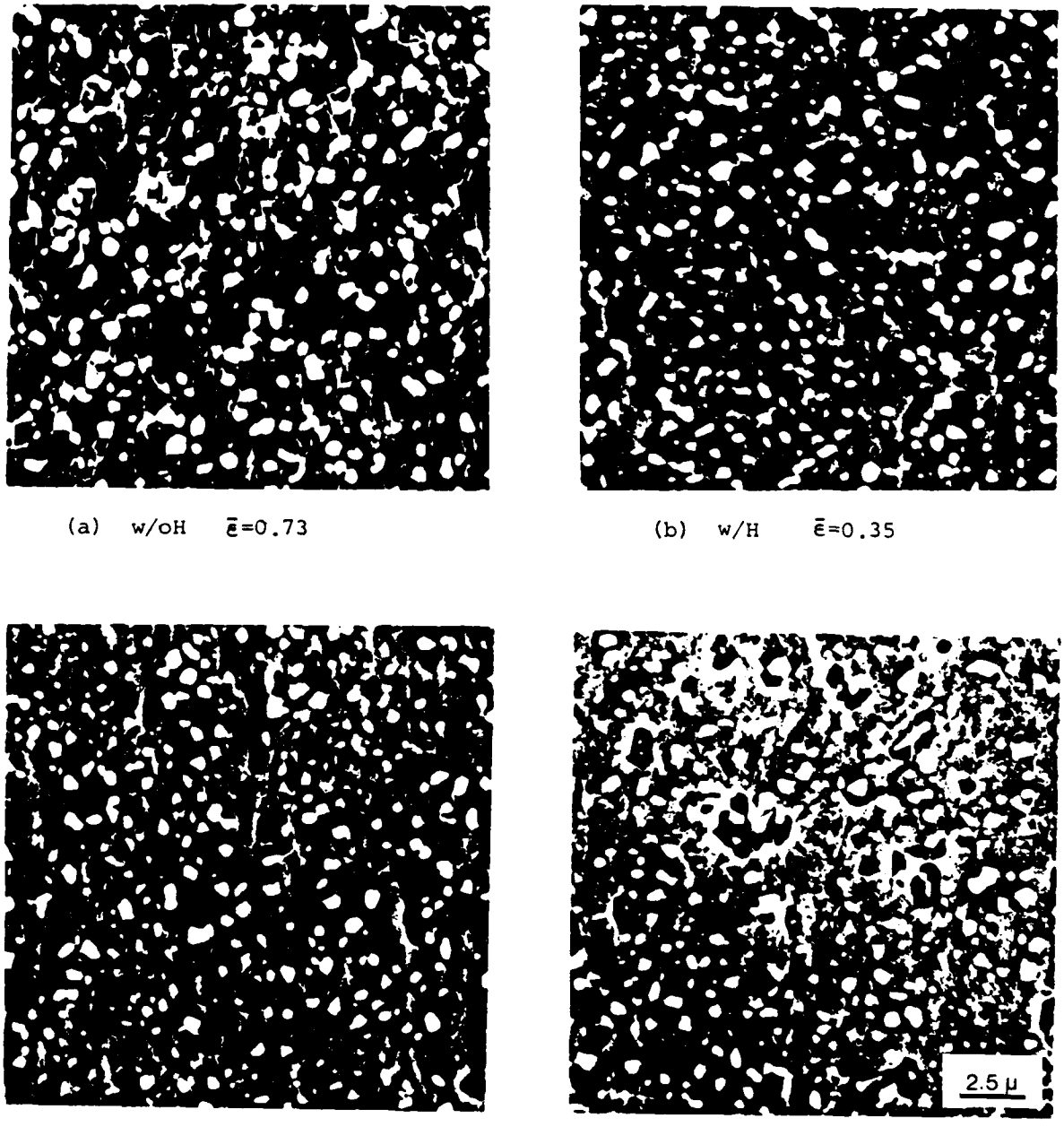

(a) w/oH $\bar{\epsilon}$=0.73

(b) w/H $\bar{\epsilon}$=0.35

(c) w/oH $\bar{\epsilon}$=1.10
(near the fracture)

(d) w/H $\bar{\epsilon}$=0.60
(near the fracture)

Figure 6: Scanning electron micrographs of sections perpendicular to the fracture showing void nucleation and void growth for equibiaxial specimens of steel AISI 1070 uncharged and charged with hydrogen; the fracture surface is horizontal.

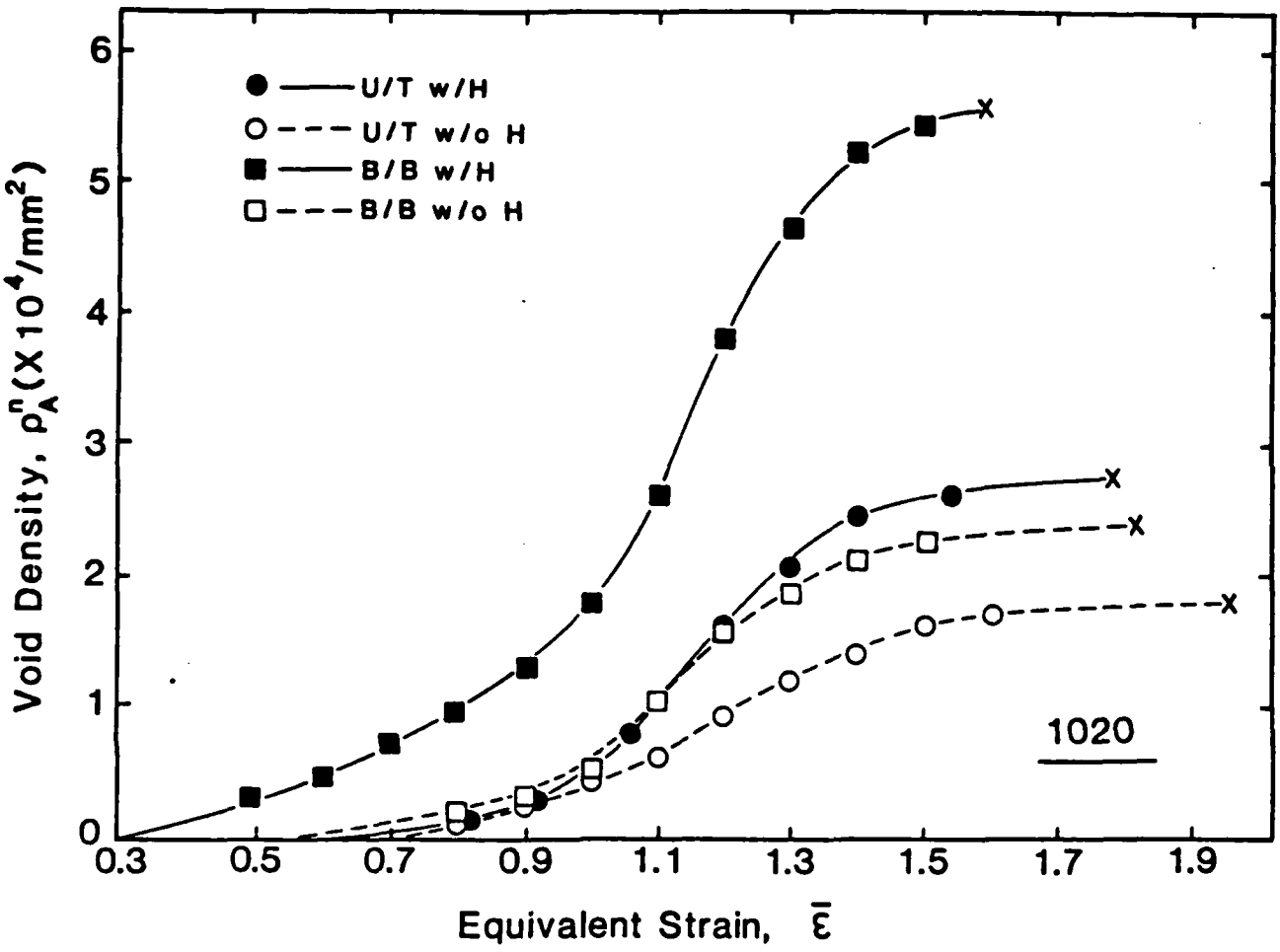

Figure 7: The dependence of void density ρ_A^n on equivalent strain for specimens of charged and uncharged spheroidized 1020 steel tested in uniaxial tension U/T and equibiaxial tension B/B.

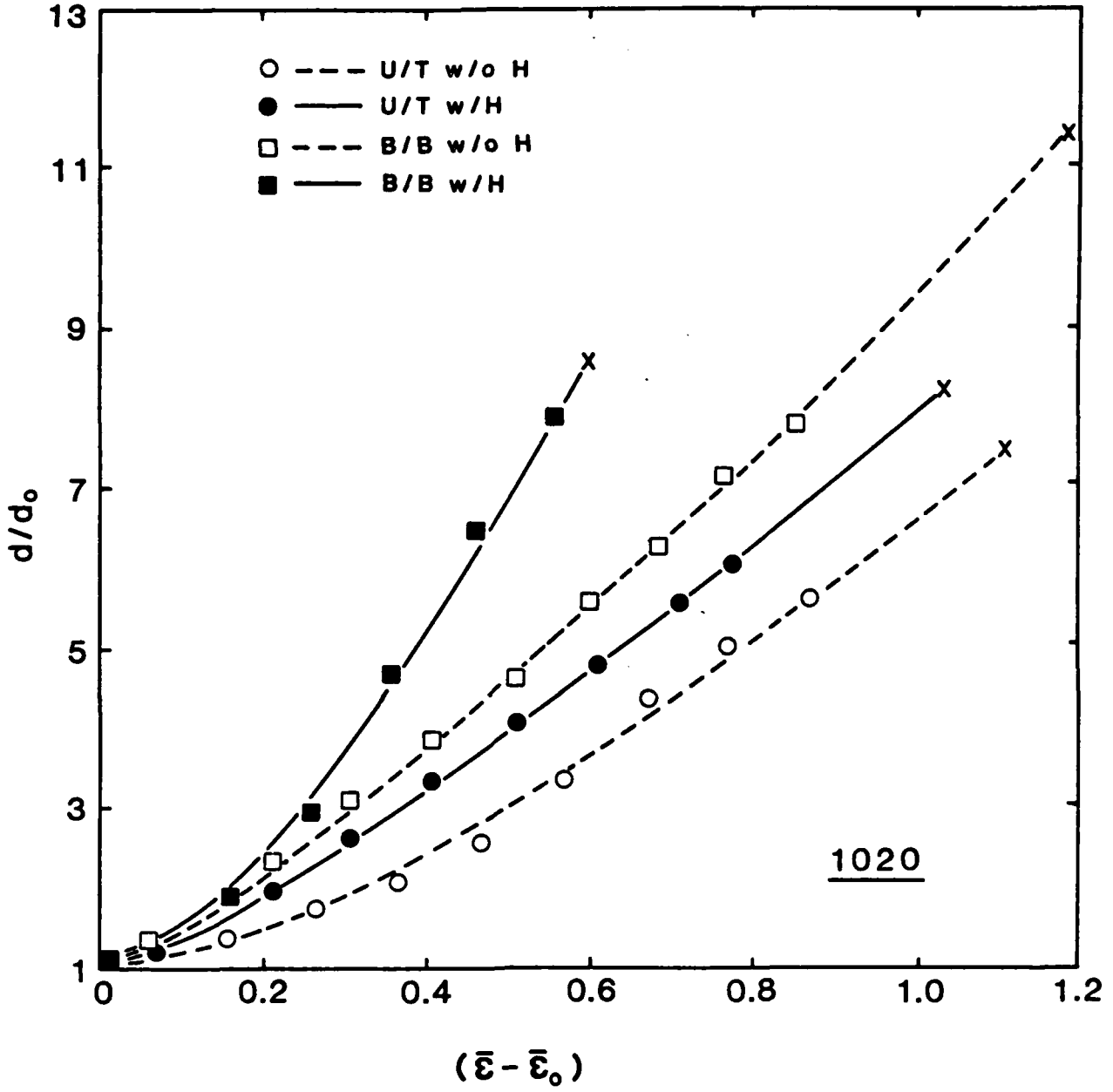

Figure 8: The ratio of the void size d at an equivalent strain $\bar{\varepsilon}$ to an initial void size d_o at a corresponding strain ε_o as a function of strain increment $(\varepsilon - \varepsilon_o)$. Data for spheroidized 1020 steel sheets tested in uniaxial U/T and equibiaxial B/B tension in either charged or uncharged conditions.

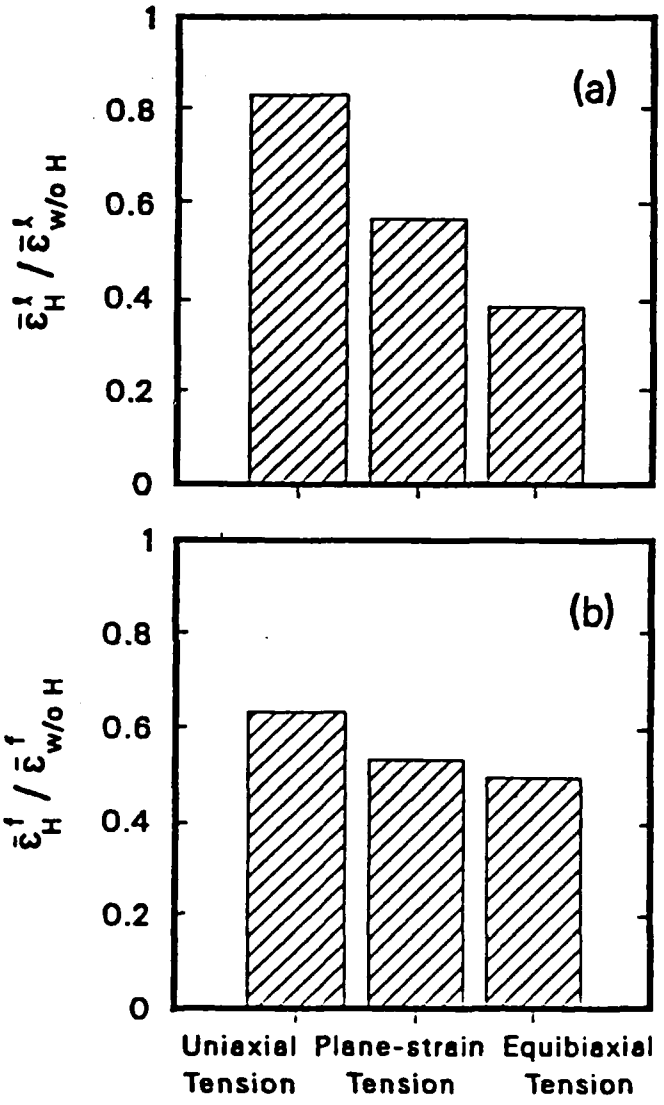

Figure 9: The normalized loss of ductility for hydrogen-charged Ni as a function of stress state at an equivalent strain rate of $1 \times 10^{-5} s^{-1}$. The equivalent strain to fracture has been determined on (a) a "limit" strain basis adjacent to the necked, failure region and (b) a "fracture" strain basis as measured at the fracture surface. After ref. 10.

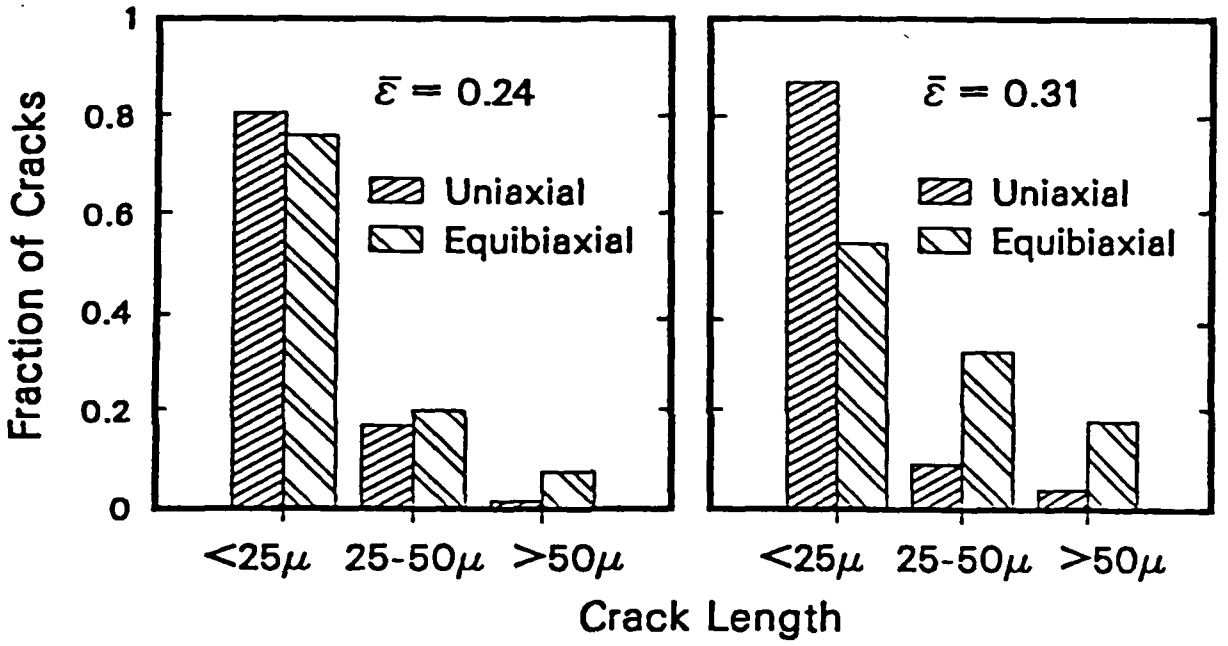

Figure 10: The fractional population of surface microcracks as a function of crack length in uniaxial vs. equibiaxial tension at equivalent shear strains of (a) 0.25 and (b) 0.31. It should be noted that the standard deviations for the data are approximately: $\pm$ 0.10 for crack lengths < 25 μm, $\pm$ 0.07 for th 25-50um cracks, and $\pm$ 0.03 for crack lengths > 50 μm. Data is for nickel after ref. 10.

END

DTIC

10—86